

# Development of poly(lactide-co-glycolide) nanoparticles functionalized with a mitochondria penetrating peptide

Francesca Selmin,<sup>a\*</sup> Giulia Magri,<sup>a</sup> Chiara G.M. Gennari,<sup>a</sup> Silvia Marchianò,<sup>b</sup> Nicola Ferri<sup>c</sup> and Sara Pellegrino<sup>d\*</sup> 

The development of mitochondria-targeting cell permeable vectors represents a promising therapeutic approach for several diseases, such as cancer and oxidative pathologies. Nevertheless, access to mitochondria can be difficult. A new hybrid material composed by poly(lactide-co-glycolide) (PLGA) functionalized with a 6-mer mitochondria penetrating peptide (MPP), consisting in alternating arginine and unnatural cyclohexylalanine, was developed. Circular dichroism, FT-IR and DSC studies indicated that the conjugation of the peptide with the polymer led to the obtainment of a more rigid material with respect to both PLGA and MPP as such. In particular, a conformational rearrangement to a helical structure was observed for MPP. MPP-PLGA conjugates were used for the preparation of nanoparticles that showed no cytotoxicity in MTT assay, suggesting their putative use for future studies on mitochondria targeting. Copyright © 2016 European Peptide Society and John Wiley & Sons, Ltd.

**Keywords:** conformational study; hybrid polymers; mitochondria penetrating peptide; nanoparticles; poly(lactide-co-glycolide); polymer-peptide

## Introduction

In the last years, nanomaterials have gained an increasing interest in a wide range of applications, from biomedicine to catalysis and electrochemistry.[1–8] Hybrid biomaterials, that is, systems created from components of at least two distinct classes of molecules, lead to new materials that possess unprecedented levels of structural organization and novel properties at molecular level.[9–12] In the pharmaceutical field, polymer-derived nano-sized drug delivery systems have been developed to enhance pharmacokinetics and metabolic stability.[13–15] In particular, the decoration of polymers with functional peptides is a powerful approach to design nanosystems able to deliver payloads directly to the cell of interest.[16,17]

The copolymers of lactic and glycolic acids (PLGA) are among the few polymers approved by the Food and Drug Administration for human clinical applications such as surgical sutures, implantable devices and drug delivery systems because of their excellent biocompatibility and biodegradability.[18] Recently, it has been reported the PLGA functionalization with different functional peptides, such as cell penetrating octa-arginine (R8) and carrier peptides.[19,20] It has been shown that polymer characteristics, as well as nanoparticle size and surface modifications, play an important role in determining the efficacy and the biodistribution of these nanocarriers. Furthermore, the nanoparticle fabrication process could also affect their efficiency and the toxicity.

In this work, we aimed to develop a new hybrid material composed by PLGA functionalized with a mitochondria-penetrating peptide, a peptide composed of alternating cationic (arginine) and apolar (cyclohexylalanine) residues (MPP).[21,22] Engineering an efficient mitochondria-targeting cell permeable vector is challenging, because of the inner membrane structure that results

impermeable against a wide range of molecules.[23] Being cationic and lipophilic at the same time, MPP is able to enter the mitochondria and, covalently linked to bioactive compounds, has been used as cellular cargo.[22] To the best of our knowledge, it has not been used for the functionalization of polymeric nanoparticles. Here, we studied the conjugation of MPP to PLGA, the effect of the polymer on peptide conformation, and we set up suitable protocols for the obtainment of nanoparticles. Finally, the cytotoxicity of the new hybrid nano-material was evaluated.

## Materials and Methods

### Materials

Fmoc Rinkamide resin, Fmoc-protected (L)-amino acids, HBTU (*N,N,N',N'*-Tetramethyl-O-(1H-benzotriazol-1-yl)uronium hexafluorophosphate), HOBt (1-Hydroxybenzotriazole hydrate) and DIPEA (*N,N*-

\* Correspondence to: Dr. Sara Pellegrino and Dr. Francesca Selmin. E-mail: sara.pellegrino@unimi.it; francesca.selmin@unimi.it

a Department of Pharmaceutical Sciences, Università degli Studi di Milano, via G. Colombo, 71, 20133, Milano, Italy

b Department of Pharmacological and Biomolecular Sciences, via Balzaretti, 9, 20133, Milano, Italy

c Department of Pharmaceutical and Pharmacological Sciences, University of Padua, Padua, Italy

d Department of Pharmaceutical Sciences, Università degli Studi di Milano, via Venezian, 21, 20133, Milano, Italy

Diisopropylethylamine) were purchased from Iris Biotech GmbH (Marktredwitz, Germany). Solvents, piperidine and other reagents were purchased from Sigma-Aldrich (Darmstadt, Germany). Uncapped poly(D,L-lactide-co-glycolide) (PLGA) [batch characteristics: lactide/glycolide mole ratio: 50:50;  $M_w = 11 \pm 0.1$  kDa;  $DI = 1.5 \pm 0.1$ ;  $T_g = 37.9 \pm 0.5$  °C] was purchased from Lakeshore Biomaterials (Birmingham, USA).

MPP was synthesized using a CEM Liberty peptide synthesizer (Matthews, NC, USA) and purified using RP-HPLC with a Jasco (Easton, MD, USA) BS-997-01 instrument and a DENALI C-18 column from GRACE VYDAC (10  $\mu$ m, 250  $\times$  22 mm; Columbia, Maryland, USA). ESI mass spectra were recorded on a LCQ Advantage spectrometer from Thermo Finnigan (Waltham, MA USA).  $^1$ H-NMR spectra were acquired on a Bruker (Millerica, MA, USA) Advance 300 Spectrometer. Circular dichroism (CD) spectra were recorded on a Jasco (Easton, MD, USA) J-810 spectropolarimeter. Infrared spectra were recorded on a FT-IR spectrometer Perkin-Elmer (Waltham, MA USA) 16 PC. The gel permeation chromatography (GPC) system consisted of two  $\mu$ Styragel<sup>TM</sup> columns connected in series (7.8  $\times$  300 mm each, one with  $10^4$  Å pores and one with  $10^3$  Å pores), delivery device (HP 1100 Series, ChemStations Hewlett Packard, Agilent Technologies, Santa Clara, USA), refractive index detector, UV/visible detector set at  $\lambda = 210$  nm and software to compute molecular weight distribution (Agilent, USA). The thermal properties of PLGA and its conjugates were characterized by a DSC 1 (Mettler Toledo, Greifensee, CH) equipped with a refrigerated cooling system. Nanoparticles were characterized by photon correlation spectroscopy (PCS) and by Phase Analysis Light Scattering (M3-PALS), using a dynamic light scatter Zetasizer Nano ZS (Malvern Instrument, Worcestershire, UK), equipped with a backscattered light detector.

### Synthesis of the Mitochondria-Penetrating Peptide (MPP)

MPP (H-Cha-Arg-Cha-Arg-Cha-Arg-NH<sub>2</sub>) was prepared by microwave-assisted solid phase synthesis [24] on Rinkamide resin (0.57 meq/g) as solid support. A fivefold molar excess of Fmoc-protected amino acids (0.2 M in N-methyl pyrrolidinone) and HOBt/HBTU/DIEA (5 : 5 : 10 eq) as activators were used. Coupling reactions were performed for 5 min at 40 W with a maximum temperature of 75 °C. Deprotection was performed twice using 20% piperidine in dimethylformamide (5 and 10 min each). Cleavage from the resin was performed using 10 ml of Reagent K (trifluoroacetic acid/phenol/water/thioanisole/1,2-ethanedithiol; 82.5 : 5 : 5 : 5 : 2.5) for 180 min. Following cleavage, the labelled peptide was precipitated and washed using ice-cold anhydrous ethyl ether. The peptide was purified by RP-HPLC using a gradient elution of 5–70% solvent B (solvent A: water/acetonitrile/trifluoroacetic acid 95 : 5 : 0.1; solvent B: water/acetonitrile/trifluoroacetic acid 5 : 95 : 0.1) over 20 min at a flow rate of 20 ml/min. The purified peptide was freeze-dried and stored at 0 °C. MPP was then analysed by ESI(+)-MS confirming the  $M_w$ :  $M_w$  calcd. 943.09;  $M_w$  found 473.81  $[(M_w + 2)/2] + 1$ , 316.27  $[(M_w + 3)/3] + 1$ .  $^1$ H-NMR (300 MHz, DMSO, T = 323 K)  $\delta$  ppm: 0.86–0.88 (m, 6H), 1.14–1.33 (m, 13H), 1.50–1.91 (m, 32H), 3.12–3.23 (m, 8H overlapped), 3.81–3.84 (m, 1H), 4.18–4.39 (m, 5H), 7.12–7.25 (m, 13H), 7.79–7.81 (m, 3H), 8.05–8.18 (m, 3H) (Figure 1).

### Preparation of MPP-PLGA Conjugates

PLGA (50 mg, 5  $\mu$ mol) was dissolved in dichloromethane (1 ml) for 1 h. HOBt and EDC HCl (Table 1) were then added, and the

suspension was stirred for 0.5 h at rt. MPP (Table 1) previously dissolved in DMF (0.5 ml) and DIPEA (Table 1) were added, and the mixture was left under stirring for 12 h at rt. Water (2 ml) was added to reaction mixture. The aqueous layer was extracted with dichloromethane (3  $\times$  2 ml). The collected organic layers were dried on Na<sub>2</sub>SO<sub>4</sub>, and the solvent was removed under vacuum affording a white solid (50 mg). MPP-PLGA conjugation was confirmed by FT-IR (KBr pellet) and  $^1$ H-NMR (DMSO-d<sub>6</sub> at 50 °C and 300 MHz). The percentage of peptide conjugation (PC) on PLGA was calculated by  $^1$ H NMR comparing the integration area of the peptide peak at about 0.9 ppm and PLGA multiplet at 5.3 ppm.

### Characterization of MPP-PLGA conjugates

#### Gel Permeation Chromatography (GPC)

The molecular weight of PLGA before and after conjugation reactions was measured by GPC. The chromatographic conditions were set as follow: tetrahydrofuran (THF) filtered with 0.45  $\mu$ m pores PTFE filter (Pall Gelman Sciences TF 450, Port Washington, USA) as mobile phase at a flow rate of 1 ml/min, injection volume of 20  $\mu$ l and temperature analysis of 25.0  $\pm$  0.1 °C. Polymer samples were dissolved in THF at a concentration of 2 mg/ml. The molecular weight weight-average ( $M_w$ ) and the molecular weight number-average ( $M_n$ ) of each sample were calculated using monodisperse polystyrene standards with  $M_w$  ranging from 947 to 42 300 Da.

#### Differential Scanning Calorimetry (DSC)

Exactly weighted polymers samples were placed into 40  $\mu$ l aluminium pans and subjected to two cooling and heating cycles from 0 °C to 80 °C at heating and cooling rates of 20 °C/min. DSC cell was purged with a dry nitrogen flow of 80 ml/min. The system was calibrated using an indium standard. Data were treated with Star<sup>e</sup> System software (Mettler Toledo, Greifensee, CH). The glass transition temperatures were measured on the second heat scan.

#### Circular Dichroism (CD)

Stock solution was prepared in acetonitrile (500  $\mu$ mol for PLGA and MPP-PLGA conjugates, 28  $\mu$ mol for MPP). Spectra were obtained from 195 to 250 nm with a 0.1 nm step and 1 s collection time per step, taking three averages. The spectrum of the solvent was subtracted to eliminate interference from cell, solvent and optical equipment. The CD spectra were plotted as mean residue ellipticity  $\theta$  (degree  $\times$  cm<sup>2</sup>  $\times$  dmol<sup>-1</sup>) versus wave length  $\lambda$  (nm). Noise reduction was obtained using a Fourier-transform filter program from Jasco (Easton, MD, USA).

### Preparation of Nanoparticles

Two different strategies were pursued to prepare MPP-PLGA nanoparticles (NPs), namely solvent displacement and emulsification-solvent evaporation. The former consisted on the polymer dissolution in 1 ml of acetonitrile at the concentration of 10 mg/ml and the addition dropwise at a constant rate to 10 ml of MilliQ<sup>®</sup> water filtered with a nylon syringe filter of 0.2  $\mu$ m nominal porosity. The system was maintained at 4  $\pm$  1 °C and stirred at 500 rpm for 15 min and, then, heated until 20  $\pm$  1 °C for 3 h.

The latter method involved the MPP-PLGA dissolution in 1 ml of dichloromethane at the concentration of 4 mg/ml. The

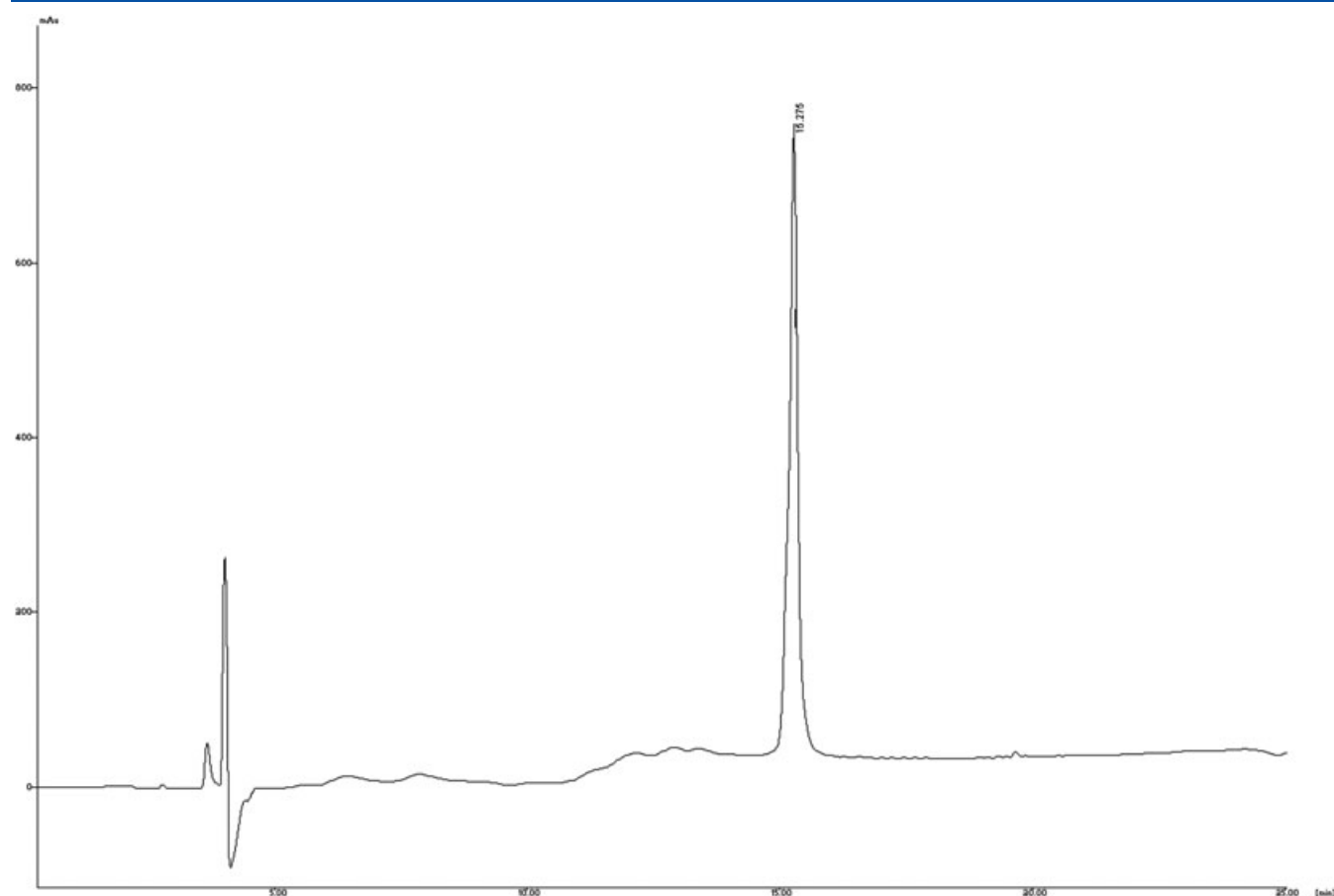


**Figure 1.** Analytical RP-HPLC spectrum of purified MPP (gradient elution of 5–70% solvent B in 30 min).

**Table 1.** Relative amounts of PLGA, peptide, coupling reagents and base used in conjugation reaction. Percentage of peptide conjugation on PLGA (PC)

	PLGA	MPP	HOBt	EDC	DIPEA	% PC
MPP-PLGA 1	5 $\mu$ mol	5 mg (5 $\mu$ mol)	4 mg (25 $\mu$ mol)	5 mg (25 $\mu$ mol)	9 $\mu$ l (50 $\mu$ mol)	30
MPP-PLGA 2	5 $\mu$ mol	15 mg (15 $\mu$ mol)	3 mg (15 $\mu$ mol)	3 mg (15 $\mu$ mol)	6 $\mu$ l (30 $\mu$ mol)	50
MPP-PLGA 3	5 $\mu$ mol	15 mg (15 $\mu$ mol)	4 mg (25 $\mu$ mol)	5 mg (25 $\mu$ mol)	9 $\mu$ l (50 $\mu$ mol)	95

solution was emulsified with 2 ml of 5% PVA 10-98 aqueous solution using an ultrasound probe set at an amplitude of 40% for 1 min in ice bath. The emulsion was finally poured into 6 ml of 0.1% PVA aqueous solution stirred at 500 rpm. The evaporation of the organic solvent was carried out over 3 h at about 25 °C.

## Characterization of NPs

The mean hydrodynamic diameter ( $D_H$ ) and the size distribution of the nanoparticles were evaluated by PSC operating at 173°. All the analyses were carried out in disposable polystyrene cuvettes at a constant temperature of 25 °C, using the polystyrene latex (RI = 1590) as reference material. The results were calculated using the Dispersion Technology Software (DTS, Malvern Instruments Ltd., Worcestershire, UK), and they are reported as intensity distribution.

The zeta potential of the nanoparticles was assessed by M3-PALS technique. The analyses were carried out into a capillary cuvette at 25 °C, with polystyrene latex as reference material.

## MTT Cytotoxicity Assay

HCT-116 cells were seeded at a density of  $4 \times 10^4$ /well in a 48 well tray and incubated with DMEM supplemented with 10% FCS; 24 h later, the medium was replaced with one containing MPP-PLGA 3 nanoparticles at increasing concentrations, and the cultures were incubated for 48 h. At the end of the incubation, the cell viability was determined by MTT assay. To this purpose, MTT (Sigma-Aldrich, Darmstadt, Germany) solution was prepared at 1.5 mg/ml in RPMI without phenol red and was filtered through a 0.2  $\mu$ m filter. Then, the culture medium was removed from the plate, and 300  $\mu$ l of MTT solution was added into each well. Cells were incubated for 2 h at 37 °C with 5% CO<sub>2</sub>, 95% air and complete humidity. After 2 h, 200  $\mu$ l of 2-propanol/0.04 N HCl was added into each well, and

the solution was resuspended. The optical density (OD) of the wells was determined using a plate reader at a wavelength of 550 nm.

## Results and Discussion

Mitochondria-penetrating peptides are synthetic cell permeable peptides that are able to enter mitochondria and are characterized by delocalized positive charge and lipophilicity. Normally, they consist in an alternating sequence of positive charged (Arg or Lys) and hydrophobic amino acids (Phe or the unnatural cyclohexylalanine, Cha). The cationic character is needed for driving the uptake of the delivery vectors through the cellular and mitochondrial membranes, both of which have a negative membrane potential. On the other hand, the passage of cations across the hydrophobic inner mitochondrial membrane is facilitated by the presence of lipophilic groups, such as benzene or cyclohexyl ring.[21,22]

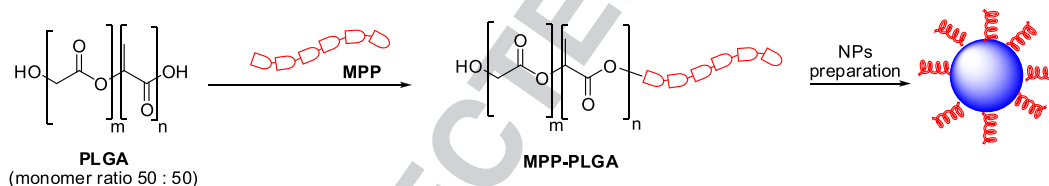
In this work, we selected the 6-mer sequence H-Cha-Arg-Cha-Arg-Cha-Arg-NH<sub>2</sub> (MPP) for the functionalization of a well-known biodegradable polymer as poly(lactide-co-glycolide) (PLGA). In particular, we decided to first conjugate MPP to PLGA and to characterize the main physico-chemical properties of the novel

material and then to study the feasibility of the preparation of nanoparticles (Scheme 1).

MPP was prepared by MW-assisted solid phase peptide synthesis following standard procedure. MPP conjugation with PLGA was carried out in dichloromethane, using HOBt and EDC HCl as coupling reagents and DIPEA as base. Different molar ratios (Table 1) were evaluated. In particular, the coupling was scarcely efficient using an equimolar ratio between PLGA and MPP and a five-fold excess of coupling reagents (MPP-PLGA 1). We then increased the amount of MPP (3 eq), and in the same time we reduced the amount of coupling reagents, yielding to MPP-PLGA 2 characterized by a 50% of PC. The best coupling conditions were obtained using a MPP/PLGA molar ratio of 3:1, a five-fold excess of coupling reagents and 10 equivalents of the base (MPP-PLGA 3, 95% of PC). The of MPP-PLGA conjugates was assessed by using <sup>1</sup>H NMR spectroscopy and by setting as diagnostic for conjugation the peptide peak at 0.9 ppm (Figure 2). In particular, we compared its area value

with that of the peak at 5.3 ppm assignable to the polymer, as already reported in the literature for other peptide-PLGA functionalization.[20]

The conjugates were also analysed by GPC to evaluate the average molecular weight of the new hybrid polymers because PLGA is a very sensitive material and several factors can modify its



**Scheme 1.** Functionalization of poly(lactide-co-glycolide) (PLGA) with MPP peptide and subsequently nanoparticles preparation.

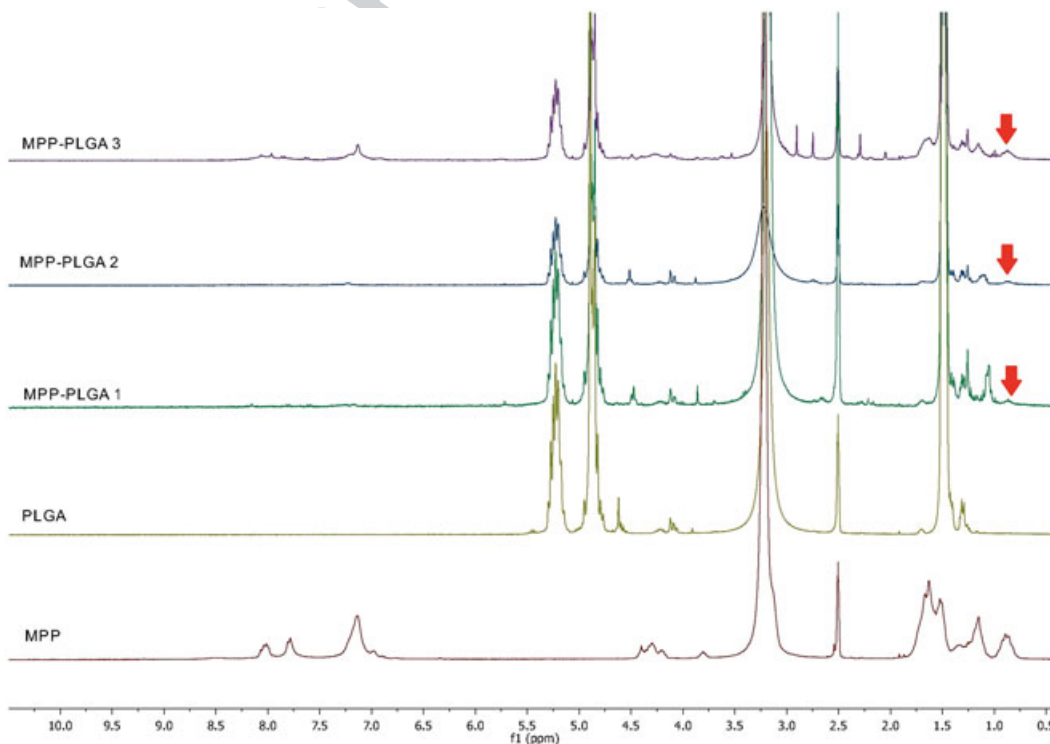


**Figure 2.** <sup>1</sup>H-NMR spectrum of MPP, PLGA and MPP-PLGA conjugates.



main physico-chemical features.[25] Moving from PLGA to its conjugates, the  $M_w$  increased from about 11.0 kDa to 13.6 kDa, confirming the  $^1\text{H-NMR}$  data and thus the conjugation of MPP to the polymer. Likewise,  $M_n$  and dispersity index of the raw PLGA and MPP-PLGA conjugates overlapped at about 7.8 kDa and 1.5, respectively, suggesting that the conjugation conditions did not have a detrimental effect on polymer main features.

For MPP-PLGA 2 and MPP-PLGA 3, the conjugation was also investigated by FT-IR analysis (Figure 3).

In both cases, the polymers were characterized by a band at  $1760\text{ cm}^{-1}$  (PLGA ester stretching), a band at around  $1656\text{ cm}^{-1}$  and a shoulder at  $1673\text{ cm}^{-1}$  (both because of MPP amide I stretching). By comparing the FT-IR spectra of MPP alone (red curve) with MPP-PLGA conjugates (black and blue curves), a shift of amide I band frequency at  $1635\text{ cm}^{-1}$  was observed, together with a decrease in intensity of the band at  $1673\text{ cm}^{-1}$ . Of relevance, a new band at  $1656\text{ cm}^{-1}$  is observed. These data suggested that a stabilization of peptide helix structure was effective upon conjugation.[26] CD analysis was thus performed. Figure 4 reports the spectra of MPP and of MPP-PLGA 3 conjugate in acetonitrile. In solution, MPP alone did not assume a preferred conformation as underlined by a negative ellipticity value at 190 nm and the low intensity of the  $n-\pi$  bands. For MPP-PLGA conjugate, a positive value at 190 nm together with negative Cotton effects at 205 nm and 220 nm of similar intensity were observed. This finding confirmed an increase of peptide helical content when MPP is bound to PLGA, and thus, an increase in the overall rigidity of the hybrid polymeric system.

Moreover, a reduction of the specific heat ( $C_p$ ) associated to the glass transition was also noticed in MPP-PLGA 3 (Table 2). Generally speaking, the decrease of  $C_p$  is related to the increase of hydrogen bonds or the weaker Van der Waals forces, limiting the molecular mobility of the polymer chains.[27] Hence, the stiffening of the polymer structure can be because of the induction of the preferred conformation of MPP which forced PLGA to a rearrangement.

Based on the results obtained, MPP-PLGA 2 and 3 were considered as suitable candidates to prepare nanoparticles. Several methods are reported in literature for the preparation of nano-sized

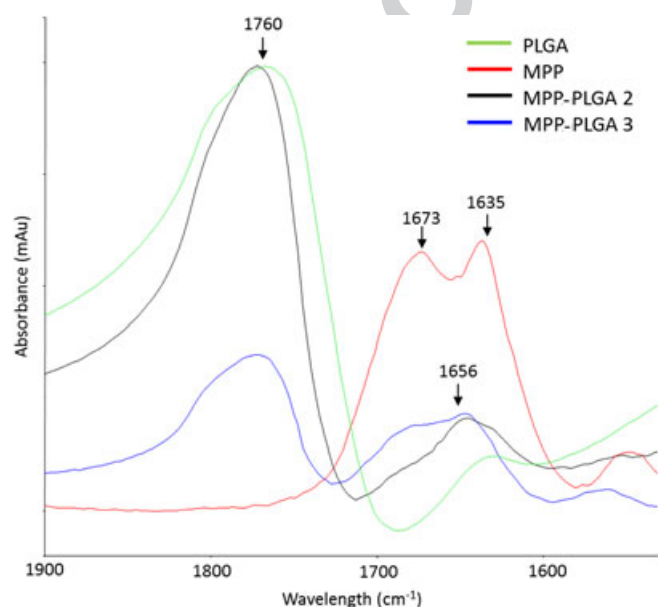


Figure 3. FT-IR spectra on KBr pellets.

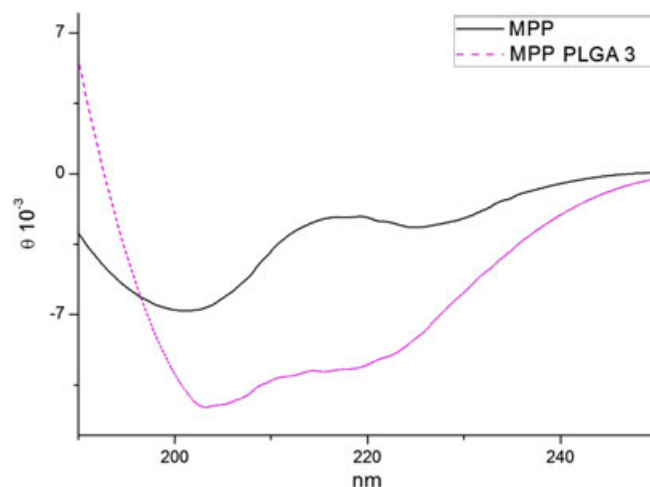


Figure 4. CD spectra of MPP alone and MPP-PLGA 3 (100  $\mu\text{mol}$  in ACN at rt).

Table 2. Main differences in terms of glass transition temperature ( $T_g$ ) and specific heat ( $C_p$ ) resulted by the thermal analysis of the raw PLGA and PLGA conjugates

Polymer ID	$T_g$ ( $^{\circ}\text{C}$ )	$C_p$ (mW/g $^{\circ}\text{C}$ )
PLGA	$37.9 \pm 0.5$	$29.1 \pm 0.8$
MPP-PLGA 2	$38.9 \pm 1.0$	$28.2 \pm 1.9$
MPP-PLGA 3	$45.8 \pm 0.2$	$22.1 \pm 2.1$

systems.[28] As a rule, an optimal method should be as simple as possible, limiting the use of excipients such as stabilizing agents that could cause toxic effects depending on their nature and amount. The solvent displacement method (also known as 'nanoprecipitation') is the most common technique reported for PLGA-based systems.[29] In a preliminary step of this work, different water-miscible organic solvents were considered for the preparation of the MPP-PLGA solution, such as acetone, acetone/absolute ethanol mixture in two volume ratios (i.e. 85/15 and 70/30) and acetonitrile. The concentration of the polymer solution was fixed at 10 mg/ml. The raw PLGA was freely soluble in all solvents reported above. The acetone only or the mixture with absolute ethanol in the ratio of 85/15 allowed solubilizing MPP-PLGA 2 at a maximum concentration of 5 mg/ml, causing the formation of NPs with a size of about 100 nm (Table 3). The conjugate did not dissolve in acetone/absolute ethanol 70/30. MPP-PLGA 2 resulted soluble at the prefixed concentration only in acetonitrile and the corresponding NPs presented a  $D_H$  of  $171 \pm 5\text{ nm}$  (Table 3).

On the other hand, MPP-PLGA 3 did not dissolve in the water-miscible solvents considered. This was probably because MPP deeply modified the physico-chemical features of the polymer. Hence, MPP-PLGA 3 was dissolved in dichloromethane in order to prepare NPs by emulsification-solvent evaporation. This method permitted the formation of NPs with a  $D_H$  of  $454 \pm 12\text{ nm}$  and a polydispersity index of  $0.451 \pm 0.082$ . More importantly, the conjugation with MPP resulted in a significant increase in the zeta potential of NPs from about  $-35\text{ mV}$  to about  $1.3 \pm 0.2\text{ mV}$ . No signs of aggregation were noticed after the preparation of MPP-PLGA 3 NPs, probably because of the presence of residual PVA on the surface of the NPs, which permitted a particle-particle repulsion.[30] The negative zeta potential of PLGA is because of the presence of negatively charged carboxylic acid end groups. Only in NPs made

**Table 3.** Hydrodynamic diameter ( $D_H$ ), polydispersity index (PDI) and zeta potential ( $\xi$ ) of NPs obtained by using MPP–PLGA 2 solutions in different water-miscible solvents

Solvent	Concentration (mg/ml)	$D_H$ (nm)	PDI	$\xi$ (mV)
Acetone	5	98 ± 2	0.101 ± 0.014	−46.2 ± 2.5
Acetone/ethanol 85/15	5	96 ± 1	0.106 ± 0.004	−45.0 ± 1.5
Acetone/ethanol 70/30	—	—	—	—
Acetonitrile	10	171 ± 5	0.100 ± 0.041	−45.4 ± 0.6

of MPP–PLGA 3, the conjugation with MPP increased the superficial charge to values near neutral. This is a further confirmation that a highest amount of positively charged MPP was linked to PLGA and was thus able to neutralize the charged carboxylic acid end groups of PLGA.

The most promising NPs obtained by MPP–PLGA 3 hybrid polymer were thus submitted to preliminary cytotoxicity studies. Cell viability was investigated in colon carcinoma cell line HCT116. As shown in Figure 5, MPP–PLGA 3 did not significantly alter the cell viability after 48 h incubation at concentrations up to 5  $\mu\text{g/ml}$ .

In conclusion, PLGA was successfully functionalized with 6-mer MPP peptide containing Arg and the unnatural amino acid Cha. By tuning MPP/PLGA molecular ratio and the coupling reagents' equivalent, it has been possible to obtain a hybrid polymer characterized by a higher conformational rigidity with respect to PLGA and MPP alone. Indeed, when linked to PLGA, MPP peptide underwent a conformational switch toward helical conformation that induced the stiffening of the overall polymeric structure. The new hybrid polymer was used to realize MPP functionalized PLGA NPs using both the solvent displacement and the emulsification-solvent evaporation methods. The obtained NPs showed no toxicity in MTT cell viability test, suggesting their potential use in pharmacological application. Future investigations will be aimed to study NP mitochondria internalization and loading ability of this new hybrid material.

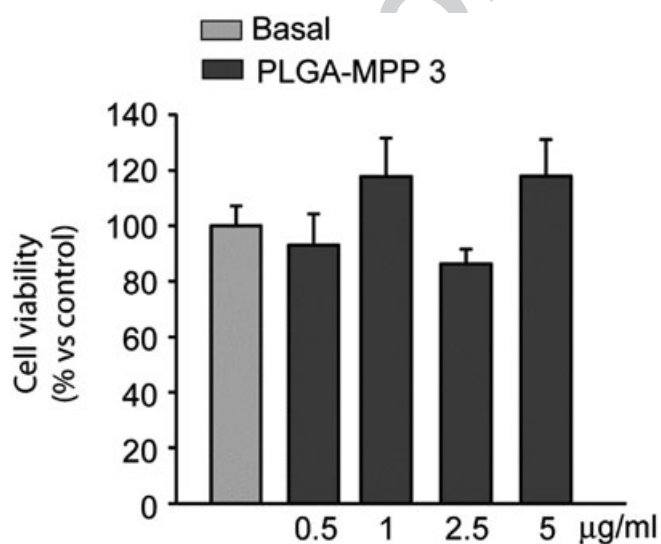


**Figure 5.** Cell viability after incubation with different concentrations of MPP–PLGA 3. HCT-116 cells were cultured for 48 h in the presence or absence of reported concentrations of PLGA–MPP 3.0, and their viability was estimated by MTT assay. Each bar represents the mean  $\pm$  standard deviation of three determinations.

## Acknowledgements

Funding for this work has been provided by Università degli Studi di Milano (Piano Sviluppo, Linea B).

## References

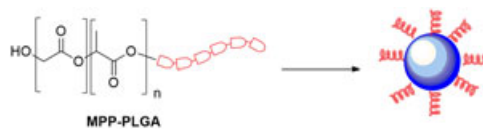
- Habibi N, Kamaly N, Memic A, Shafiee H. Self-assembled peptide-based nanostructures: smart nanomaterials toward targeted drug delivery. *Nano Today* 2016; **11**: 41. DOI: 10.1016/j.nantod.2016.02.004.
- Blum AP, Kammeyer JK, Rush AM, Callmann CE, Hahn ME, Gianneschi NC. Stimuli-responsive nanomaterials for biomedical applications. *J. Am. Chem. Soc.* 2015; **137**: 2140. DOI: 10.1021/ja510147n.
- Irvine DJ, Hanson MC, Rakhra K, Tokatlian T. Synthetic nanoparticles for vaccines and immunotherapy. *Chem. Rev.* 2015; **115**: 11109. DOI: 10.1021/acs.chemrev.5b00109.
- Bonetti A, Pellegrino S, Das P, Yuran S, Bucci R, Ferri N, Meneghetti F, Castellano C, Reches M, Gelmi ML. Dipeptide nanotubes containing unnatural fluorine-substituted  $\beta(2,3)$ -diarylamino acid and L-alanine as candidates for biomedical applications. *Org. Lett.* 2015; **17**: 4468. DOI: 10.1021/acs.orglett.5b02132.
- Maione S, Gil AM, Fabregat G, del Valle LJ, Triguero J, Laurent A, Jacquemin D, Estrany F, Jiménez AI, Zanuy D, Catiaviela C, Alemán C. Electroactive polymer–peptide conjugates for adhesive biointerfaces. *Biomater. Sci.* 2015; **3**: 1395. DOI: 10.1039/C5BM00160A.
- Torabi SF, Lu Y. Functional DNA nanomaterials for sensing and imaging in living cells. *Curr. Opin. Biotech.* 2014; **28**: 88. DOI: 10.1016/j.copbio.2013.12.011.
- Zhang L, Qin L, Wang X, Cao H, Liu M. Supramolecular chirality in self-assembled soft materials: regulation of chiral nanostructures and chiral functions. *Adv. Mater.* 2014; **26**: 6959. DOI: 10.1002/adma.201305422.
- Xu Y, Zhang B. Recent advances in porous Pt-based nanostructures: synthesis and electrochemical applications. *Chem. Soc. Rev.* 2014; **43**: 2439. DOI: 10.1039/C3CS60351B.
- He C, Liu D, Lin W. Nanomedicine applications of hybrid nanomaterials built from metal–ligand coordination bonds: nanoscale metal–organic frameworks and nanoscale coordination polymers. *Chem. Rev.* 2015; **115**: 11079. DOI: 10.1021/acs.chemrev.5b00125.
- Cobo I, Li M, Sumerlin BS, Perrier S. Smart hybrid materials by conjugation of responsive polymers to biomacromolecules. *Nat. Mater.* 2015; **14**: 43. DOI: 10.1038/nmat4106.
- Murase SK, Haspel N, del Valle LJ, Perpète EA, Michaux C, Nussinov R, Puiggali J, Alemán C. Molecular characterization of L-phenylalanine terminated poly(L-lactide) conjugates. *RSC Adv.* 2014; **4**: 23231. DOI: 10.1039/C4RA01534G.
- Sanchez C, Belleville P, Popall M, Nicole L. Applications of advanced hybrid organic–inorganic nanomaterials: from laboratory to market. *Chem. Soc. Rev.* 2011; **40**: 696. DOI: 10.1039/C0CS00136H.
- Nicolas J, Mura S, Brambilla D, Mackiewicz N, Couvreur P. Design, functionalization strategies and biomedical applications of targeted biodegradable/biocompatible polymer-based nanocarriers for drug delivery. *Chem. Soc. Rev.* 2013; **42**: 1147. DOI: 10.1039/c2cs35265f.
- Sapsford E, Algar WR, Berti L, Boeneman Gemmill K, Casey BJ, Oh E, Stewart MH, Medintz IL. Functionalizing nanoparticles with biological molecules: developing chemistries that facilitate nanotechnology. *Chem. Rev.* 2013; **113**: 1904. DOI: 10.1021/cr300143v.
- Farokhzad OC, Langer R. Impact of nanotechnology on drug delivery. *ACS Nano* 2009; **3**: 16. DOI: 10.1021/nn900002m.
- Chen B, He X-Y, Yi X-Q, Zhuo R-X, Cheng S-X. Dual-peptide-functionalized albumin-based nanoparticles with pH-dependent self-

- assembly behavior for drug delivery. *ACS Appl. Mater. Interfaces* 2015; **7**: 15148. DOI: 10.1021/acsami.5b03866.
- 17 Malhotra M, Prakash S. Targeted drug delivery across blood-brain-barrier using cell penetrating peptides tagged nanoparticles. *Curr. Nanosci.* 2011; **7**: 81. DOI: 10.2174/157341311794480336.
- 18 Anderson JM, Shive MS. Biodegradation and biocompatibility of PLA and PLGA microspheres. *Adv. Drug Del. Rev.* 2012; **64**: 72. DOI: 10.1016/j.addr.2012.09.004.
- 19 O'Donnell A, Moollan A, Baneham S, Ozgul M, Pabari RM, Cox D, Kirby BP, Ramtoola Z. Intranasal and intravenous administration of octa-arginine modified poly(lactic-co-glycolic acid) nanoparticles facilitates central nervous system delivery of loperamide. *J. Pharm. Pharmacol.* 2014; **67**: 525. DOI: 10.1111/jphp.12347.
- 20 Colzani B, Biagiotti M, Speranza G, Dorati R, Modena T, Conti B, Tomasi C, Genta I. Smart biodegradable nanoparticulate materials: poly-lactide-co-glycolide functionalization with selected peptides. *Curr. Nanosci.* 2016; **12**: 347.
- 21 Horton KL, Stewart KM, Fonseca SB, Guo Q, Kelley SO. Mitochondria-penetrating peptides. *Chem. Biol.* 2008; **15**: 375. DOI: 10.1016/j.chembiol.2008.03.015.
- 22 Yousif LF, Stewart KM, Horton KL, Kelley SO. Mitochondria-penetrating peptides: sequence effects and model cargo transport. *ChemBioChem* 2009; **10**: 2081. DOI: 10.1002/cbic.200900017.
- 23 Jean SR, Tulumello DV, Wisnovsky SP, Lei EK, Pereira MP, Kelley SO. Molecular vehicles for mitochondrial chemical biology and drug delivery. *ACS Chem. Biol.* 2014; **9**: 323. DOI: 10.1021/cb400821p.
- 24 Pellegrino S, Annoni C, Contini A, Clerici F, Gelmi ML. Expedient chemical synthesis of 75mer DNA binding domain of MafA: an insight on its binding to insulin enhancer. *Amino Acids* 2012; **43**: 1995. DOI: 10.1007/s00726-012-1274-2.
- 25 Selmin F, Blasi P, DeLuca PP. Accelerated polymer biodegradation of risperidone poly(D, L-lactide-co-glycolide) microspheres. *AAPS PharmSciTech* 2012; **13**: 1465. DOI: 10.1208/s12249-012-9874-4.
- 26 Kong J, Yu S. Fourier transform infrared spectroscopic analysis of protein secondary structures. *Acta Biochim. Biophys. Sin.* 2007; **39**: 549. DOI: 10.1111/j.1745-7270.2007.00320.x.
- 27 Gibbs JH, Di Marzio EA. Nature of the glass transition and the glassy state. *J. Chem. Phys.* 1958; **28**: 373. DOI: 10.1063/1.1744141.
- 28 Lai P, Daeer W, Löbenberg R, Prenner EJ. Overview of the preparation of organic polymeric nanoparticles for drug delivery based on gelatine, chitosan, poly(D,L-lactide-co-glycolic acid) and polyalkylcyanoacrylate. *Colloids Surf. B* 2014; **118**: 154. DOI: 10.1016/j.colsurfb.2014.03.017.
- 29 Fessi H, Puisieux F, Devissaguet JP, Ammoury N, Benita S. Nanocapsule formation by interfacial polymer deposition following solvent displacement. *Int. J. Pharm.* 1989; **55**, R1: . DOI: 10.1016/0378-5173(89)90281-0.
- 30 Quintanar-Guerrero D, Ganem-Quintanar A, Allémann E, Fessi H, Doelker E. Influence of the stabilizer coating layer on the purification and freeze-drying of poly(D, L-lactic acid) nanoparticles prepared by an emulsion-diffusion technique. *J. Microenc.* 1998; **15**: 107. DOI: 10.3109/02652049809006840.

## Special Issue Article

### Development of poly(lactide-co-glycolide) nanoparticles functionalized with a mitochondria penetrating peptide

Francesca Selmin, Giulia Magri, Chiara G.M. Gennari, Silvia Marchianò, Nicola Ferri and Sara Pellegrino



A new hybrid material composed by poly(lactide-co-glycolide) (PLGA) functionalized with a 6-mermitochondria penetrating peptide (MPP) was developed. A conformational to a helical structure was observed for MPP upon conjugation with the polymer. This new rigid material was used for the preparation of cell compatible nanoparticles.



# Author Query Form

---

**Journal: Journal of Peptide Science**




**Article: psc\_2952**

Dear Author,

During the copyediting of your paper, the following queries arose. Please respond to these by annotating your proofs with the necessary changes/additions.

- If you intend to annotate your proof electronically, please refer to the E-annotation guidelines.
- If you intend to annotate your proof by means of hard-copy mark-up, please use the standard proofing marks. If manually writing corrections on your proof and returning it by fax, do not write too close to the edge of the paper. Please remember that illegible mark-ups may delay publication.

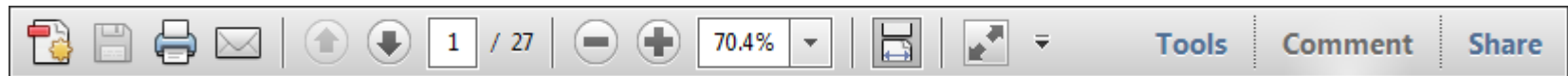
Whether you opt for hard-copy or electronic annotation of your proofs, we recommend that you provide additional clarification of answers to queries by entering your answers on the query sheet, in addition to the text mark-up.

Query No.	Query	Remark
Q1	AUTHOR: Please confirm that given names (red) and surnames/family names (green) have been identified correctly.	
Q2	AUTHOR: Figure 1 was not cited in the text. An attempt has been made to insert the figure into a relevant point in the text – please check that this is OK. If not, please provide clear guidance on where it should be cited in the text.	
Q3	AUTHOR: Revised figure 1 still contains small and poor quality of text.	

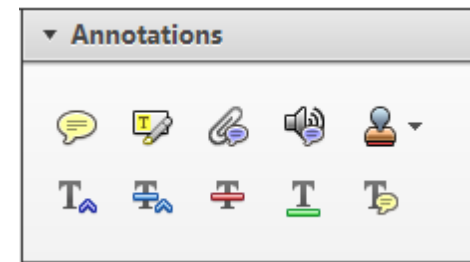
Required software to e-annotate PDFs: **Adobe Acrobat Professional** or **Adobe Reader** (version 7.0 or above). (Note that this document uses screenshots from **Adobe Reader X**)

The latest version of Acrobat Reader can be downloaded for free at: <http://get.adobe.com/uk/reader/>

Once you have Acrobat Reader open on your computer, click on the **Comment** tab at the right of the toolbar:



This will open up a panel down the right side of the document. The majority of tools you will use for annotating your proof will be in the **Annotations** section, pictured opposite. We've picked out some of these tools below:



**1. Replace (Ins) Tool – for replacing text.**

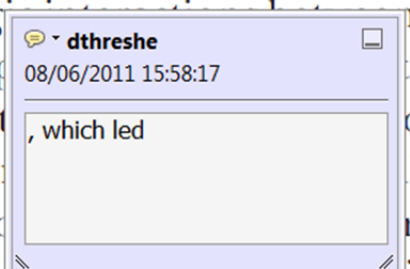


Strikes a line through text and opens up a text box where replacement text can be entered.

**How to use it**

- Highlight a word or sentence.
- Click on the **Replace (Ins)** icon in the Annotations section.
- Type the replacement text into the blue box that appears.

standard framework for the analysis of microeconomics. Nevertheless, it also led to the emergence of a new paradigm of strategic behaviour. The number of competitors in the industry is that the structure of the main components of the model, are exogenous. An important work on this by Shirasaka (henceforth) we open the 'black b



**2. Strikethrough (Del) Tool – for deleting text.**



Strikes a red line through text that is to be deleted.

**How to use it**

- Highlight a word or sentence.
- Click on the **Strikethrough (Del)** icon in the Annotations section.

there is no room for extra profits and the number of firms are zero and the number of firms (net) values are not determined by Blanchard and ~~Kiyotaki~~ (1987), perfect competition in general equilibrium of aggregate demand and supply in a classical framework assuming monopoly. An exogenous number of firms

**3. Add note to text Tool – for highlighting a section to be changed to bold or italic.**



Highlights text in yellow and opens up a text box where comments can be entered.

**How to use it**

- Highlight the relevant section of text.
- Click on the **Add note to text** icon in the Annotations section.
- Type instruction on what should be changed regarding the text into the yellow box that appears.

dynamic responses of mark-ups consistent with the VAR evidence

sation... y Ma... and... on n... to a... stent also with the demand-



**4. Add sticky note Tool – for making notes at specific points in the text.**



Marks a point in the proof where a comment needs to be highlighted.

**How to use it**

- Click on the **Add sticky note** icon in the Annotations section.
- Click at the point in the proof where the comment should be inserted.
- Type the comment into the yellow box that appears.

and supply shocks. Most of the... number... standard fr... cy. Nev... le of str... ber of competitors and the imp... is that the structure of the secto



USING e-ANNOTATION TOOLS FOR ELECTRONIC PROOF CORRECTION

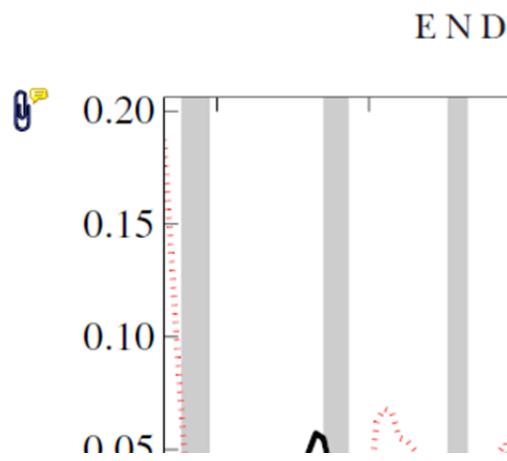
**5. Attach File Tool – for inserting large amounts of text or replacement figures.**



Inserts an icon linking to the attached file in the appropriate place in the text.

**How to use it**

- Click on the [Attach File](#) icon in the Annotations section.
- Click on the proof to where you'd like the attached file to be linked.
- Select the file to be attached from your computer or network.
- Select the colour and type of icon that will appear in the proof. Click OK.



**6. Add stamp Tool – for approving a proof if no corrections are required.**

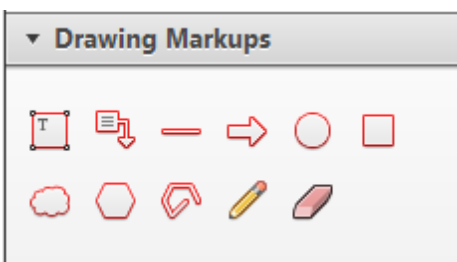


Inserts a selected stamp onto an appropriate place in the proof.

**How to use it**

- Click on the [Add stamp](#) icon in the Annotations section.
- Select the stamp you want to use. (The [Approved](#) stamp is usually available directly in the menu that appears).
- Click on the proof where you'd like the stamp to appear. (Where a proof is to be approved as it is, this would normally be on the first page).

of the business cycle, starting with the  
 on perfect competition, constant ret  
 production. In this environment goods  
 extra profits and the number of firms  
 he number of firms is determined by  
 determined by the model. The New-Key  
 otaki (1987), has introduced produc  
 general equilibrium models with nomin  
 ed and supply shocks. Most of this literat

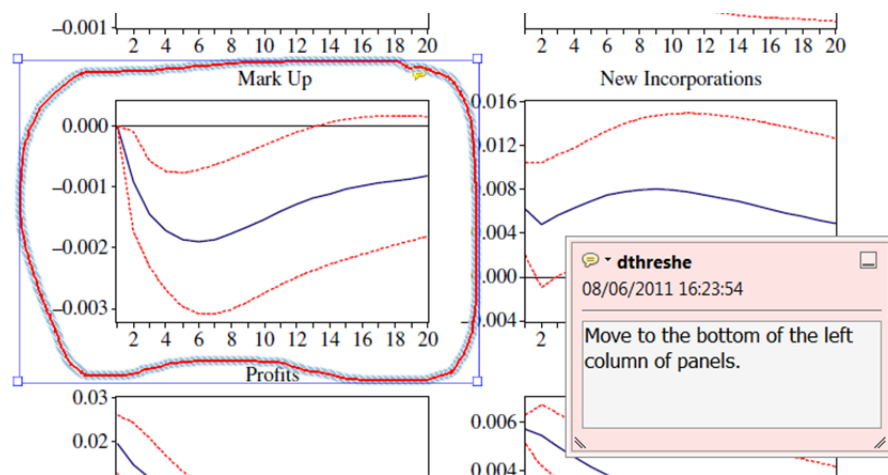


**7. Drawing Markups Tools – for drawing shapes, lines and freeform annotations on proofs and commenting on these marks.**

Allows shapes, lines and freeform annotations to be drawn on proofs and for comment to be made on these marks..

**How to use it**

- Click on one of the shapes in the [Drawing Markups](#) section.
- Click on the proof at the relevant point and draw the selected shape with the cursor.
- To add a comment to the drawn shape, move the cursor over the shape until an arrowhead appears.
- Double click on the shape and type any text in the red box that appears.



For further information on how to annotate proofs, click on the [Help](#) menu to reveal a list of further options:

